

Confidence Based Anisotropic Filtering of Magnetic Resonance Images

Ersin Bayram¹, Yaorong Ge², Christopher L. Wyatt¹

¹: Department of Medical Engineering, School of Medicine ²: Department of Computer Science
Wake Forest University, NC, USA

Abstract— Image filtering is an important off-line image processing technique to improve the signal-to-noise ratio (SNR) and/or contrast-to-noise ratio (CNR) of acquired images. The major drawback of filtering is that it often blurs the fine structures and object boundaries in the image along with noise. Anisotropic diffusive filtering techniques incorporate gradient information to blur homogeneous regions while preserving the boundaries and interesting structures. Unfortunately, their performance is limited in low contrast regions and around fuzzy boundaries. This paper introduces a multi-scale confidence based conductance function to address the limitations of anisotropic diffusive filtering. Experiments on phantom and magnetic resonance (MR) images have been performed using both our method and the gradient-based anisotropic diffusive filtering for comparison purposes.

Keywords— anisotropic diffusion, filtering, scale selection, conductance, confidence, MR imaging

I. INTRODUCTION

Despite significant improvements in recent years, MR images often suffer from low SNR or CNR, especially in cardiac and brain imaging. This is problematic for further tasks such as segmentation of important features, 3D image reconstruction and registration. Therefore, noise reduction techniques is of great interest in MR imaging as well as in other imaging modalities.

Noise reduction techniques can be categorized in two groups: acquisition-based noise reduction methods and post-acquisition image filtering. Acquisition-based methods generally utilize longer scan times, averaging over repeated measurements, enlarging the voxel volume that is being employed or improvements in hardware. Beside hardware improvements, these methods either increase image acquisition time or sacrifice spatial resolution. Hence, post-acquisition image filtering stands as an inexpensive and effective alternative.

Post-acquisition filtering techniques can be further divided into two groups: space-invariant filtering and space-variant filtering. In space-invariant filtering, spatially independent smoothing is applied to the whole image data such as low-pass filtering or neighborhood averaging [1]. However, space-invariant filtering methods blur the important features in the image along with the noise.

Space-variant filtering techniques aim to address this limitation by using local, feature-dependent strategies. The approaches include recursive low-pass filtering with adaptive coefficients [2], linear least-squares error filtering [3], local shape-adaptive template filtering [4], and anisotropic diffusive filtering [5].

A. Anisotropic Diffusion

Anisotropic diffusive filtering is based on multi-scale representation of images. Multi-scale filtering has been formally introduced by Witkin [6]. The idea is embedding the original image, $I_0(x, y)$, in a family of derived images, $I(x, y, \sigma)$, obtained by convolving $I_0(x, y)$ with a Gaussian kernel, $G(x, y, \sigma)$, of varying variance, σ^2 :

$$I(x, y, \sigma) = I_0(x, y) * G(x, y, \sigma) \quad (1)$$

Koenderink [7] has showed that this one parameter family of derived images can be represented as the solution of the heat conduction or *diffusion* equation:

$$I_\sigma = c\nabla^2 I(x, y) \quad (2)$$

with $I(x, y, 0) = I_0(x, y)$ as the initial condition and the constant, c being the conductance coefficient. Perona and Malik [5] treated the conductance coefficient as a scale and space varying function, $c(x, y, t)$, forcing the diffusion process to respect the natural boundaries of objects. This leads to the *anisotropic diffusion* equation:

$$I_\sigma = \text{div}(c(x, y, \sigma)\nabla I(x, y)) = c\nabla^2 I + \nabla c\nabla I \quad (3)$$

Perona and Malik proposed two different conductance functions each monotonically decreasing functions of the magnitude of the gradient of the intensity:

$$c(x, y, \sigma) = e^{-\left(\frac{|\nabla I|}{K}\right)^2} \quad (4)$$

$$c(x, y, \sigma) = \frac{1}{1 + \left(\frac{|\nabla I|}{K}\right)^2} \quad (5)$$

These conductance functions weaken the diffusion process for values of the the intensity gradient greater than parameter K , encouraging intra- rather than inter-region diffusion. However, these conductance functions have drawbacks: fine structures in low SNR or CNR regions often disappear and fuzzy boundaries are further blurred. To address these issues, noise level and edge-strength based K selection [8] as well as adaptive schemes [9] have been proposed. Moreover, there has been significant research on determining a better conductance function such as knowledge-based approaches [10].

This paper proposes a new method for defining the conductance function using *a-priori* knowledge and a scale selection mechanism. The method, which is referred to as the *confidence-based anisotropic diffusion*, treats the conductance function as a statistically defined, gradient-based multi-scale confidence of region homogeneity.

Report Documentation Page

Report Date 25 Oct 2001	Report Type N/A	Dates Covered (from... to) -
Title and Subtitle Confidence Based Anisotropic Filtering of Magnetic Resonance Images	Contract Number	
	Grant Number	
	Program Element Number	
Author(s)	Project Number	
	Task Number	
	Work Unit Number	
Performing Organization Name(s) and Address(es) Department of Medical Engineering School of Medicine Wake Forest University, NC	Performing Organization Report Number	
Sponsoring/Monitoring Agency Name(s) and Address(es) US Army Research, Development & Standardization Group (UK) PSC 802 Box 15 FPO AE 09499-1500	Sponsor/Monitor's Acronym(s)	
	Sponsor/Monitor's Report Number(s)	
Distribution/Availability Statement Approved for public release, distribution unlimited		
Supplementary Notes In Supplementary notes put: Papers from 23rd Annual International Conference of the IEEE Engineering in Medicine and Biology Society, October 25-28, 2001, held in Istanbul, Turkey. See also ADM001351 for entire conference on cd-rom.		
Abstract		
Subject Terms		
Report Classification unclassified	Classification of this page unclassified	
Classification of Abstract unclassified	Limitation of Abstract UU	
Number of Pages 4		

II. METHODOLOGY

Any point in an image is either in a homogeneous region or on a slope of a blurred edge. A generous diffusion ($c(x, y, \sigma) \simeq 1$) is desirable in homogeneous regions as opposed to conservative diffusion ($c(x, y, \sigma) \simeq 0$) on a slope of a blurred edge. As the edge locations are unknown, a binary conductance function is not possible.

Therefore, the gradient is used as the image feature of interest in our method as well. In contrast, it is used as a tool to derive the confidence of being in a homogeneous region at each point in an image rather than an end-product to define the conductance function. The reason is that gradient strength is not a measure of the significance of a feature in the image. Low contrast and fuzzy boundaries should also be respected during the diffusion process.

A multi-scale approach is necessary in the gradient calculation as the relevant features in images exist over multiple scales. Elder and Zucker [11] proposed a method to select a minimum reliable scale at each point in an image based on *a-priori* knowledge of:

1. The noise comes from a stationary, zero-mean white noise process.
2. The standard deviation of the noise can be estimated from the image itself or by calibration.

Reliable scale means that in gradient-based edge detection, the false positive error rate due to noise alone is less than or equal to a predetermined threshold at that scale. The above assumptions are valid for MR image data. Therefore, Elder and Zucker's *minimum reliable scale* technique can be utilized in the conductance function derivation.

A. Gradient Response of Noise

The gradient computation from discrete data is an ill-posed problem. Smoothing the data with a Gaussian filter is a well-known regularization approach. Hence, the gradient can be estimated using the steerable Gaussian first derivative basis filters:

$$g_x(x, y, \sigma_1) = \frac{-x}{2\pi\sigma_1^4} e^{-\frac{(x^2+y^2)}{2\sigma_1^2}} \quad (6)$$

$$g_y(x, y, \sigma_1) = \frac{-y}{2\pi\sigma_1^4} e^{-\frac{(x^2+y^2)}{2\sigma_1^2}} \quad (7)$$

σ_1 denotes the scale of the Gaussian kernel, $g(x, y, \sigma_1)$. The gradient of the intensity function $I(x, y)$ is given by:

$$\nabla I = \cos(\theta)I_x(x, y, \sigma_1) + \sin(\theta)I_y(x, y, \sigma_1) \quad (8)$$

where

$$\theta = \arctan\left(\frac{I_y(x, y, \sigma_1)}{I_x(x, y, \sigma_1)}\right) \quad (9)$$

θ is the gradient vector direction at (x, y) . $I_x(x, y, \sigma_1)$ and $I_y(x, y, \sigma_1)$ are defined as:

$$I_x(x, y, \sigma_1) = g_x(x, y, \sigma_1) * I(x, y) \quad (10)$$

$$I_y(x, y, \sigma_1) = g_y(x, y, \sigma_1) * I(x, y) \quad (11)$$

In images, the gradient in homogeneous regions will have a non-zero response as a result of noise. In order to talk about the confidence on region homogeneity, one has to consider the likelihood of the gradient response due to noise only. Considering the derivative operation as a random process transformation, the pdf of the absolute value of the the noise gradient can be represented as [12], [11]:

$$p_{|\nabla I|}(v) = \frac{v}{s_1^2} e^{-\frac{v^2}{2s_1^2}} \quad (12)$$

where s_1 is a function of the standard deviation of the noise (σ_n) and the scale of the Gaussian kernel (σ_1):

$$s_1 = \frac{\sigma_n}{2\sqrt{2\pi}\sigma_1^2} \quad (13)$$

B. Conductance Function

Given the probability distribution function (pdf) of the gradient of the noise in Eq.12, a type 1 error (α_p) is defined when using a gradient threshold (T) to detect an edge:

$$\alpha_p = \int_T^\infty \frac{v}{s_1^2} e^{-\frac{v^2}{2s_1^2}} dv \quad (14)$$

Based on the the white noise assumption, pixel-wise type 1 error (α_p) can be related to the type 1 error for the whole image (α_I) as follows:

$$\alpha_I = 1 - (1 - \alpha_p)^N \quad (15)$$

where N is the total number of pixels in the image. Using a fixed type 1 error rate (i.e. $\alpha_I = 0.01$), we can define a *critical threshold* function using Eq.14:

$$T(\sigma_1) = \frac{\sigma_n}{2\sigma_1^2} \sqrt{\frac{-\ln(\alpha_p)}{\pi}} \quad (16)$$

Given a pointwise type 1 error of α_p , $T(\sigma_1)$ represents the statistically reliable minimum gradient response based on sensor noise and operator scale.

Fig.1.(a) and (b) are plots of $T(\alpha_I)$ for different noise levels and different type 1 error rates, respectively. $T(\sigma_1)$ is a monotonically decreasing function of σ_1 , enabling the detection of blurred boundaries, which have larger scale content than sharp boundaries. Furthermore, it is linearly proportional to the standard deviation of noise. As noise content increases, the threshold levels also increase to eliminate spurious edges.

Using a linearly sampled scale space ($\sigma_1 \in \{1, 1.5, 2, \dots\}$), a *critical threshold* map ($C(x, y)$) is defined based on the multi-scale gradient response of the intensity function:

$$C(x, y) = \max\{T(\sigma_1) : |\nabla I| \geq T(\sigma_1)\} \quad (17)$$

Fig.2.(a) is a brain MR image and Fig.2.(b) is the corresponding *critical threshold* map. In the threshold map, white regions correspond to the highest threshold level indicating the presence of a strong gradient. In black regions, the gradient response is not strong enough to use

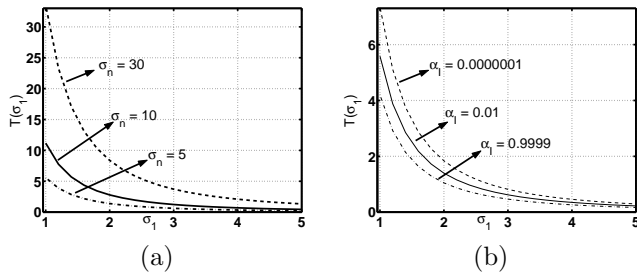


Fig. 1. (a) $T(\sigma_1)$ for different values of σ_n , $\alpha_I = 0.01$ (b) $T(\sigma_1)$ for different values of α_I , $\sigma_n = 10$

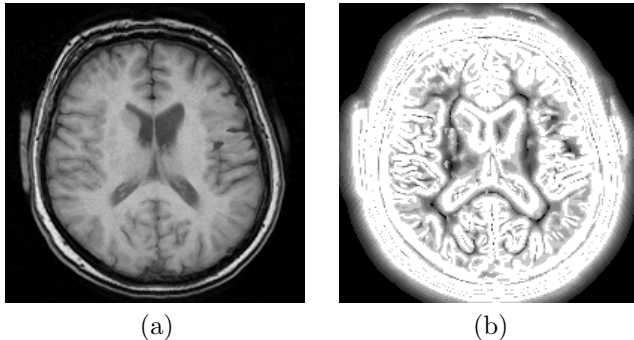


Fig. 2. (a) Brain MR Image (b) Corresponding Critical Threshold Map

any level of threshold to decide on existence of an edge, indicating a 100% confidence on region homogeneity. A conductance function for the anisotropic diffusion can be defined based on the critical threshold map:

$$c(x, y, \sigma_1) = \frac{T(\min(\sigma_1)) - C(x, y)}{T(\min(\sigma_1))} \quad (18)$$

If the gradient response of a point falls outside the sampling range of the critical threshold function, it is assumed to be homogeneous, and a conductance value of 1 is assigned to that point.

III. RESULTS

A qualitative comparison between the anisotropic diffusion method by Perona and Malik and the proposed *confidence based anisotropic diffusion* is presented using MR images and a computer generated phantom.

Fig.3.(a) is the conductance function derived from the Fig.2.(b). Black represents the zero conductance, whereas white means a conductance of 1. Fig.3.(b) shows the result of the confidence based anisotropic filtering, while Fig.3.(c) and (d) represent the anisotropic diffusion results using conductance functions in Eq.4 and Eq.5, respectively. The confidence-based filtering seems to preserve the fine details and boundaries better than the anisotropic diffusion while achieving a good smoothness in homogeneous regions such as white matter.

Fig.4 shows a region of interest (ROI) from Fig.2.(a), and diffusive filtering of this ROI using the confidence based method and the gradient-based anisotropic diffusive filtering.

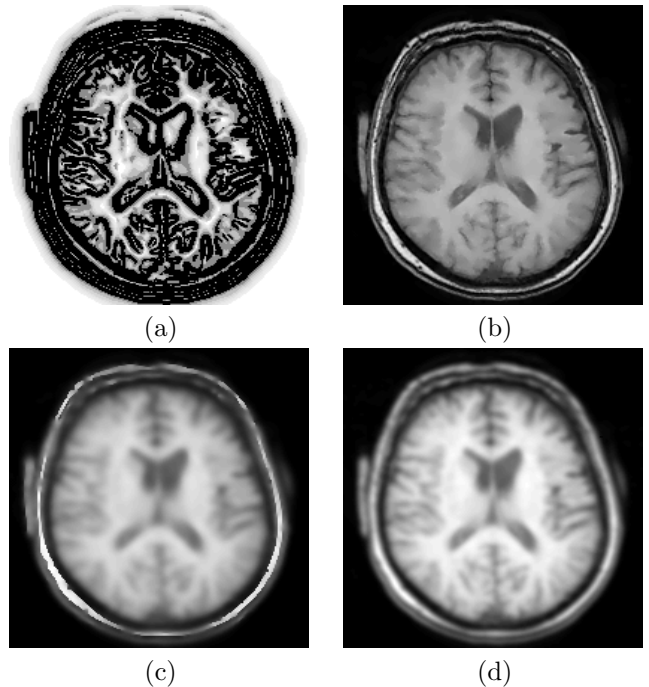


Fig. 3. (a) Confidence based conductance function corresponding to Fig.2.(a). (b) Confidence based diffusion filtering of Fig.2.(a) after 10 iterations. ((c),(d)) Anisotropic diffusive filtering after 10 iterations using Eq.4 and Eq.5, respectively

Fig.5 shows the Shepp-Logan phantom before degradation, after degradation, the confidence based conductance map, a profile through the conductance map as indicated with the solid line, and the results of the proposed and anisotropic diffusive filtering methods after 10 iterations. Both methods fail to recover the three small ellipses properly because of the low contrast boundaries in a noisy environment.

The algorithm takes around 15 seconds to run for a 256x256 image on a 333MHz Intel Pentium II processor for 10 iterations. Because the region homogeneity confidence map derivation is reliable based on the type 1 error thresholds and the additive noise assumption, the same conductance function is used at every iteration. If a new confidence map is derived at every iteration, the computation time increases by a factor of six despite no visual improvement in the result. The code is optimized by separating the 2D Gaussian kernel convolutions into two 1D convolutions.

IV. DISCUSSION

Wiener filter restoration, followed by a difference operator is used to estimate the standard deviation of the noise based on the additive noise assumption. Simulation studies show that a 5×5 Wiener filter gives an estimate of noise within a 5% error margin.

A careful examination of the conductance map in the brain MR image reveals that a wide band of zero conductance region is seen around blurred boundaries. In order to blend these regions without allowing a generous blur-

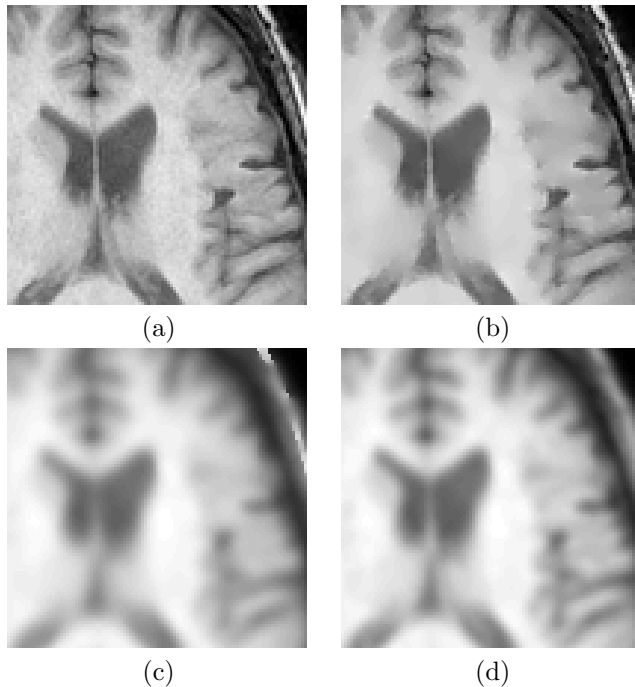


Fig. 4. (a)Region of interest from Fig.2.(a). (b) Confidence based diffusion filtering after 10 iterations. ((c),(d)) Anisotropic diffusive filtering after 10 iterations using Eq.4 and Eq.5, respectively

ring, a small constant can be added to the conductance function. A better approach will be incorporating the second derivative information into the conductance function. As edges are defined at the zero-crossings of the second derivative response, the strength of the second derivative response can be used as a measure of distance to a boundary. Unfortunately, in discrete domain, edges generally fall off-pixel locations. Thus, second derivative strength would not be a quite reliable measure, unless interpolation and sub-sampling are employed.

REFERENCES

- [1] R.E. Woods R.C. Gonzales, *Digital Image Processing*, Addison-Wesley Publishing Company, Inc., USA, 1993.
- [2] K. Rank; R. Unbehauen, "An adaptive recursive 2-d filter for removal of gaussian noise in images," *IEEE Transactions on Image Processing*, vol. 1, pp. 431–436, 1992.
- [3] P. Chan; J.S. Lim, "One-dimensional processing for adaptive image restoration," *IEEE Transactions on Acoustics, Speech, and Signal Processing*, vol. 33, pp. 117–126, 1985.
- [4] C.B. Ahn; Y.C. Song; D.J. Park, "Adaptive template filtering for signal-to-noise ratio enhancement in magnetic resonance imaging," *IEEE Transactions on Medical Imaging*, vol. 18, pp. 549–556, 1999.
- [5] P. Perona; J. Malik, "Scale-space and edge detection using anisotropic diffusion," *IEEE Transactions on Pattern Analysis and Machine Intelligence*, vol. 12, pp. 629–639, 1990.
- [6] A. P. Witkin, "Scale space filtering," in *Proceedings International Joint Conference on Artificial Intelligence*, August 1983, pp. 1019–1021.
- [7] Jan J. Koenderink, "The structure of images," *Biological Cybernetics*, vol. 50, pp. 363–370, 1984.
- [8] G. Gerig; O. Kubler; R. Kikinis; F.A. Jolesz, "Nonlinear anisotropic filtering of mri data," *IEEE Transactions on Medical Imaging*, vol. 11, no. 2, pp. 221–232, JULY 1992.
- [9] M. Sramek I. Bajla, "Improvement of 3d visualization of the brain using anisotropic diffusion smoothing of mr data," in *Proceedings of MEDINFO95- The 8th World Congress on Medical Informatics*, 1995, pp. 683–686.

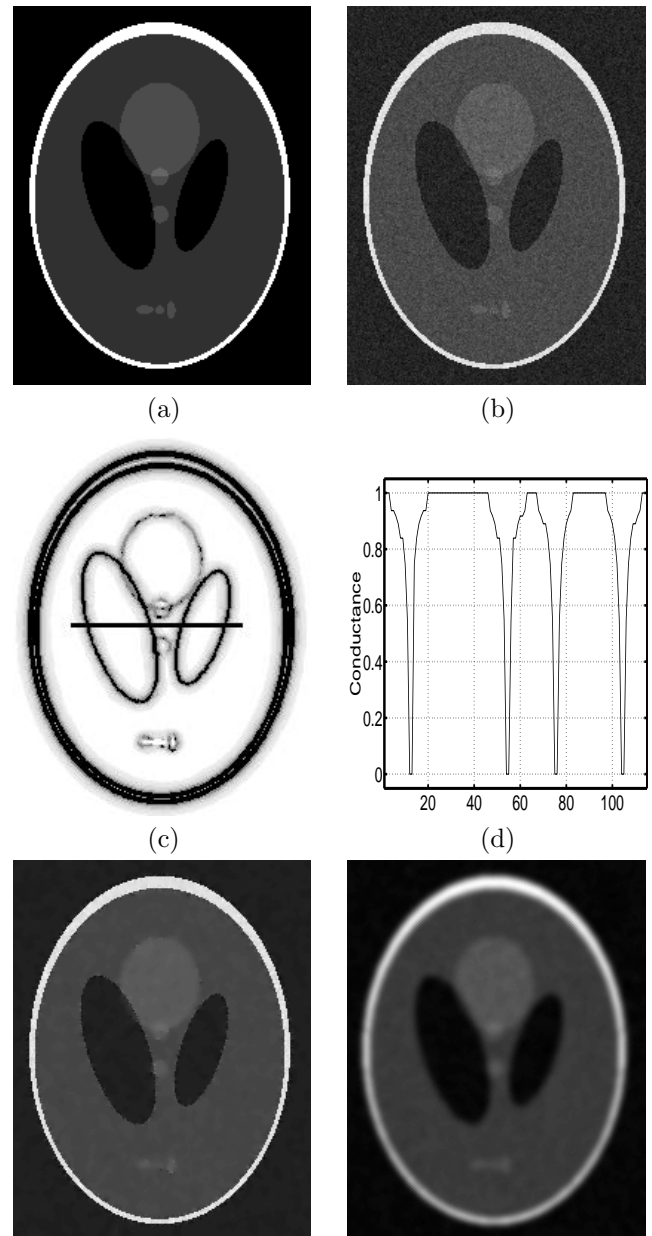


Fig. 5. (a) Shepp-Logan phantom. (b) Phantom after adding the Gaussian noise. (c) The confidence based conductance function. (d) Profile from the conductance function through the solid line. (e) Confidence based diffusion filtering result after 10 iterations. (f) Anisotropic diffusion filtering result after 10 iterations.

- [10] G.I. Sanchez-Ortiz; D. Rueckert; P. Burger, "Knowledge-based tensor anisotropic diffusion of cardiac magnetic resonance images," *Medical Image Analysis*, vol. 3, no. 2, pp. 1–25, 1999.
- [11] James H. Elder and Steven W. Zucker, "Local scale control for edge detection and blur estimation," *IEEE Trans. Pattern Analysis and Machine Intelligence*, vol. 20, no. 7, pp. 699–716, JULY 1998.
- [12] E. Bayram, "Scale selection for medical image segmentation," M.S. thesis, Wake Forest University, Winston-Salem, NC, December 2000.